View metadata, citation and similar papers at core.ac.uk
brought to you by CORE
provided by Lirias

Eur. Phys. J. A **44**, 355–361 (2010)
DOI 10.1140/epja/i2010-10945-7

THE EUROPEAN PHYSICAL JOURNAL A

Regular Article – Experimental Physics

Coulomb excitation of the odd-odd isotopes ^{106,108}In

A. Ekström[1,a], J. Cederkäll[1,2], C. Fahlander[1], M. Hjorth-Jensen[3], T. Engeland[3], A. Blazhev[4], P.A. Butler[5], T. Davinson[6], J. Eberth[4], F. Finke[4], A. Görgen[7], M. Górska[8], A.M. Hurst[5], O. Ivanov[9], J. Iwanicki[10], U. Köster[2,11], B.A. Marsh[12,13], J. Mierzejewski[10,14], P. Reiter[4], S. Siem[15], G. Sletten[16], I. Stefanescu[9], G.M. Tveten[2,15], J. Van de Walle[2,9], D. Voulot[13], N. Warr[4], D. Weisshaar[4], F. Wenander[13], and M. Zielińska[7,10]

[1] Physics Department, University of Lund, Box 118, SE-221 00 Lund, Sweden
[2] PH Department, CERN 1211, Geneva 23, Switzerland
[3] Physics Department and Center of Mathematics for Applications, University of Oslo, Norway
[4] Institute of Nuclear Physics, University of Cologne, Germany
[5] Oliver Lodge Laboratory, University of Liverpool, UK
[6] Department of Physics and Astronomy, University of Edinburgh, UK
[7] CEA Saclay, Service de Physique Nucléaire, Gif-sur-Yvette, France
[8] Gesellschaft für Schwerionenforschung, Darmstadt, Germany
[9] Instituut voor Kern- en Stralingsfysica, K.U. Leuven, Belgium
[10] Heavy Ion Laboratory, University of Warsaw, Poland
[11] Institut Laue Langevin, 6 rue Jules Horowitz, 38042 Grenoble, France
[12] Department of Physics, University of Manchester, UK
[13] AB Department, CERN 1211, Geneva 23, Switzerland
[14] Institute of Experimental Physics, University of Warsaw, Poland
[15] Department of Physics, University of Oslo, Norway
[16] Physics Department, University of Copenhagen, Denmark

Received: 30 November 2009 / Revised: 19 January 2010
Published online: 20 April 2010 – © Società Italiana di Fisica / Springer-Verlag 2010
Communicated by J. Äystö

Abstract. The low-lying states in the odd-odd and unstable isotopes ^{106,108}In have been Coulomb excited from the ground state and the first excited isomeric state at the REX-ISOLDE facility at CERN. With the additional data provided here the $\pi g_{9/2}^{-1} \otimes \nu d_{5/2}$ and $\pi g_{9/2}^{-1} \otimes \nu g_{7/2}$ multiplets have been re-analyzed and are modified compared to previous results. The observed γ-ray de-excitation patterns were interpreted within a shell model calculation based on a realistic effective interaction. The agreement between theory and experiment is satisfactory and the calculations reproduce the observed differences in the excitation pattern of the two isotopes. The calculations exclude a 6^+ ground state in ^{106}In. This is in agreement with the conclusions drawn using other techniques. Furthermore, based on the experimental results, it is also concluded that the ordering of the isomeric and ground state in ^{108}In is inverted compared to the shell model prediction. Limits on $B(E2)$ values have been extracted where possible. A previously unknown low-lying state at 367 keV in ^{106}In is also reported.

1 Introduction

The low-lying states in ^{106,108}In can be interpreted as the coupling of a proton (π) hole in the $g_{9/2}$ orbit to the neutron (ν) states in the corresponding ^{107,109}Sn isotopes [1,2]. Here we aim to expand the knowledge of the low-lying energy spectrum in ^{106,108}In using Coulomb excitation for the first time. According to measurements of the magnetic dipole moment in ^{108}In [3–5], the 7^+ ground state and the $T_{1/2} = 39.6$ min isomeric 2^+ state are dominated by the $\pi g_{9/2}^{-1} \otimes \nu d_{5/2}$ configuration. The higher-lying states have previously been identified in terms of the $\pi g_{9/2}^{-1} \otimes \nu d_{5/2}$ and $\pi g_{9/2}^{-1} \otimes \nu g_{7/2}$ multiplets [5] based on the observed decay pattern following the ^{108}Cd(p, nγ)^{108}In reaction. In ^{106}In the identification of the states is less clear. According to refs. [3,4,6] the 7^+ ground state has a dominating $\pi g_{9/2}^{-1} \otimes \nu d_{5/2}$ configuration. The first excited state in ^{106}In is also isomeric with $T_{1/2} = 5.2$ min. However, the spin measurements are inconsistent. For instance, (p, nγ) measurements report this state as a 3^+ state [7], while decay studies suggest a spin and parity of 2^+ [8,9].

It is well known that the γ-ray decay pattern following, *e.g.*, a compound reaction is largely governed by the

[a] e-mail: andreas.ekstrom@nuclear.lu.se

yrast sequence, whereas for β-decay it depends on the nature of the initial state of the parent nucleus. In Coulomb excitation the excited states are populated from below. The probability to populate a state is determined by the reduced transition matrix element for the initial and final states. Therefore, for the case at hand, this method offers the possibility to investigate the $\pi^{-1} \otimes \nu$ multiplets starting from a specific initial state that couples to the higher-lying excited states in a manner different from the techniques used before.

In the following the data is interpreted using a two-step approach. First, the spectrum of the low-energy states in the two isotopes was calculated in the shell model. The results of this calculation, including the transition probabilities, were used as input to the coupled-channels Coulomb excitation code GOSIA [10]. Secondly, the de-excitation patterns simulated in this way were compared to the corresponding experimental observations. From this, the $\pi^{-1} \otimes \nu$ multiplet character of some of the excited states could be inferred. It should be noted that the shell model interaction used here reproduces the energy spectrum of ^{106}In and ^{108}In well.

2 Experimental technique

The measurements were carried out at the REX-ISOLDE facility using RIBs consisting of both Sn and In isotopes. The results for the Sn isotopes have been published, see ref. [11]. The definition of the physical events and the offline data analysis for the present case is identical to that of the Sn experiment and therefore treated very briefly here. The In isotopes were produced by bombarding a LaC_x target with 1.4 GeV protons. The produced species effused into an ion cavity where the In isotopes were singly ionized through surface ionization against the cavity walls. Singly charged isotopes were subsequently extracted from the cavity by an applied electric field and the mass of interest was selected using electromagnetic separation. The low-energy RIB was post-accelerated to a final energy of 2.8 MeV/u and bombarded onto a 2.0 mg/cm^2 thick ^{58}Ni target. At this beam energy the inelastic collision process was safe in the meaning that the target and the projectile nuclei did not penetrate their mutual Coulomb barrier. Scattered beam and target particles were detected in a double-sided silicon strip detector (DSSSD) [12]. The γ-rays were detected by the MINIBALL spectrometer [13] which consists of 24 highly segmented Ge detectors surrounding the secondary ^{58}Ni target in a spherical configuration. Particle-γ events were time-correlated by a 100 ns gate applied in the particle-γ coincidence spectrum.

3 The observed γ-ray de-excitation patterns

The Doppler-corrected γ-ray energy spectra and the extracted γ-ray yields for ^{108}In and ^{106}In are shown in figs. 1, 2 and tables 1, 2. All but three γ-ray transitions observed in ^{106}In could be assigned to known levels in this nucleus whereas all of the observed γ-ray transitions in ^{108}In are known from before, see fig. 3. It can be noted that the branching ratios of the 283 keV and 216 keV transitions from the 4^+ state at 482 keV in ^{108}In differ from the previously measured values [5]. The 151 keV γ-ray yield in ^{108}In is the sum of the yields from the $(5)^+ \rightarrow (6,7,8)$ and $7^+ \rightarrow 7^+_{gs}$ transitions. One of the 151 keV transitions originates from a $(5)^+$ state with a known 248 keV $(5)^+ \rightarrow 7^+_{gs}$

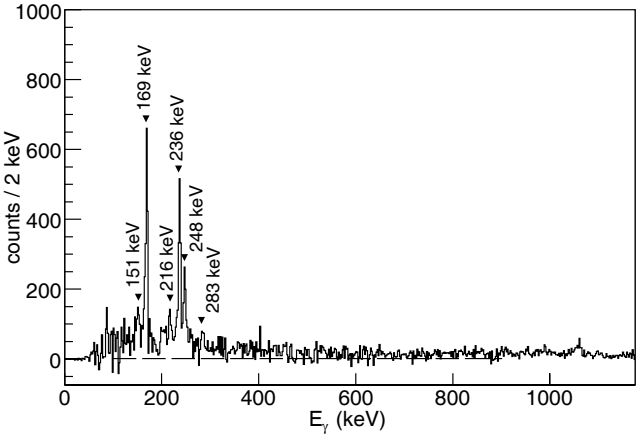

Fig. 1. Doppler-corrected γ-ray energy spectrum for ^{108}In showing the decay of the levels populated in Coulomb excitation.

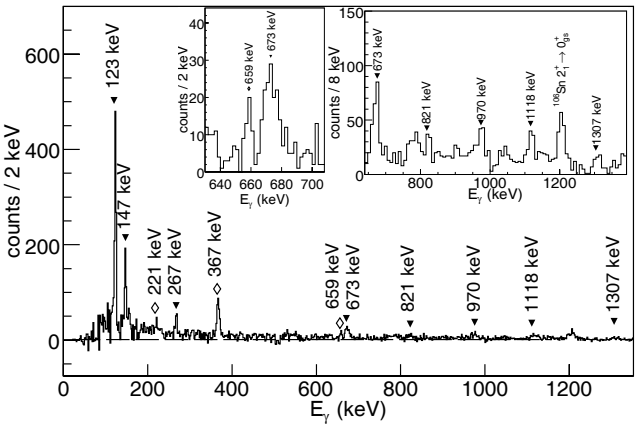

Fig. 2. Doppler-corrected γ-ray energy spectrum for ^{106}In showing the decay of the levels populated in Coulomb excitation. The transitions indicated with empty diamonds were detected for the first time in this work.

Table 1. Yields and relative intensities of the observed γ-ray transitions in ^{108}In. The γ-ray yields of the 151 keV transitions (Nos. 1 and 4) are separated using the known branching ratio of the 151 keV and 248 keV transitions from the $(5)^+$ state at 248 keV [5].

No.	Transition	E_γ (keV)	Yield	I_γ
1	$7^+ \rightarrow 7^+_{gs}$	151	377(66)	23(4)
2	$3^+ \rightarrow 2^+$	169	1536(64)	100(4)
3	$(5)^+ \rightarrow 7^+_{gs}$	248	631(50)	50(5)
4	$(5)^+ \rightarrow (6,7,8)$	151	79(14)	5(1)
5	$3^+ \rightarrow 2^+$	236	1106(67)	86(6)
6	$4^+ \rightarrow 3^+$	283	192(60)	17(5)
7	$4^+ \rightarrow 3^+$	216	150(50)	11(4)

Table 2. Yields and relative intensities of the observed γ-ray transitions in ^{106}In. The two yields given for the 123 keV doublet transition correspond to the yield of the observed γ-ray peak.

No.	Transition	E_γ (keV)	Yield	I_γ
1	$(6^+7^+8^+9^+) \rightarrow 7^+_{\rm gs}$	123	897(41)	100(5)
2	$(7^+) \rightarrow 7^+_{\rm gs}$	147	566(61)	68(8)
3	$(2)^+ \rightarrow (2)^+$	123	897(41)	100(5)
4	$(6^+) \rightarrow 7^+_{\rm gs}$	367.1(2)	321(29)	64(6)
5	$(6^+) \rightarrow (7^+)$	221.1(14)	38(14)	6(2)
6	$6 \rightarrow (6^+7^+8^+9^+)$	267	105(21)	17(4)
7	$(8^+) \rightarrow 7^+_{\rm gs}$	821	59(16)	18(5)
8	$(8^+) \rightarrow (7^+)$	673	128(24)	36(7)
9	$(8^+) \rightarrow 7^+_{\rm gs}$	1118	66(23)	25(9)
10	$(8^+) \rightarrow (7^+)$	970	81(21)	28(7)
11	$(9)^+ \rightarrow 7^+_{\rm gs}$	1307	40(12)	17(5)
12	not placed	658.7(4)	42(11)	12(3)

branch [5]. From this, the 151 keV doublet was resolved, see table 1. The yield of the 123 keV γ-ray transition in ^{106}In is also a doublet. It is the sum of the $(2)^+ \rightarrow (2)^+$ and $(6^+, 7^+, 8^+, 9^+) \rightarrow 7^+_{\rm gs}$ transitions. However, a separation similar to that in ^{108}In was not possible. Three previously unknown γ-ray transitions at 221.1(14), 367.1(2) and 658.7(4) keV were detected in ^{106}In. The 367 keV γ-ray peak is rather prominent, see fig. 2. The low probability for multiple Coulomb excitation favors a direct excitation from the $7^+_{\rm gs}$ state to a $(5^+, 6^+, 7^+, 8^+, 9^+)$ state at 367.1(2) keV. According to the shell model calculations, see sect. 3.1, this state likely has spin and parity 6^+. From the energy sums, the 221.1(14) keV γ-ray peak was placed as an 18(7)% decay branch from the 367 keV state to the (7^+) state at 147.2 keV. This further strengthens the existence of a state at 367 keV. The weak 658.7 keV transition, see table 2, could not be placed.

3.1 Shell-model–based GOSIA simulations

From inspection of the experimental de-excitation patterns of ^{106}In and ^{108}In shown in fig. 3, one can conclude that the states at higher energy couple more strongly to the 7^+ ground state in ^{106}In than in ^{108}In. In order to investigate this further a set of theoretical $E2$ and $M1$ transition matrix elements were derived using a realistic effective interaction [14] based on a G-matrix renormalized CD-Bonn nucleon-nucleon potential [15]. The model space included the orbits $\nu(1g_{7/2}, 2d_{5/2}, 3s_{1/2}, 2d_{3/2})$ and $\pi(1g_{9/2}, 2p_{1/2})$ outside the ^{88}Sr core. The single-particle energies were taken from ref. [16], the effective charges were set to $e_\pi = 1.5\,$e and $e_\nu = 1.0\,$e, and the standard gyromagnetic ratios were used. The negative-parity orbit $\nu(1h_{11/2})$ was excluded for computational gain since it has a very small amplitude in the wave functions that describe the low-energy positive-parity states. The transition matrix element were then used to simulate the γ-ray yield using the coupled-channels code GOSIA [10]. The simulation included the geometry of the setup, the thickness of the target foil, and the theoretical internal conversion coefficients [17].

The shell model calculation for ^{106}In predicts a 6^+ ground state instead of the previously experimentally assigned 7^+ ground state. In addition, in order for the GOSIA simulations to reproduce the coupling to the higher-lying states the 6^+ ground state must be replaced by the theoretical first excited 7^+_1 state. Indeed, a GOSIA simulation based on a 6^+ ground state leads to an intense $8^+_1 \rightarrow 7^+_1$ transition and only one transition to the ground state, namely from the 7^+_1 state. However, experimentally other transitions are observed as well which corroborates the 7^+_1 shell model state as the ground state. The 1307 keV state was tentatively assigned as 9^+ in ref. [18]. Most likely, it corresponds to the 9^+ state at 1271 keV in the shell model calculation. The observed decay of the (8^+) state at 821 keV has two branches, one to the 7^+ ground state and the other to the (7^+) state at 147 keV. The shell model calculation predicts a similar transition between an 8^+ state and the 7^+ ground state. However, the branch to the second 7^+ state is not reproduced. Nevertheless, the tentative 8^+ assignment seems plausible.

The simulated γ-ray intensities for transitions to the isomeric 2^+ state and the 7^+ ground state in ^{108}In are consistent with data if the isomeric fraction of the indium component of the RIB is 50%, see fig. 4. However, the current analysis is independent of the exact beam composition although the isomeric fraction of the RIB can be resolved using the γ-rays following the decay of the beam particles implanted at the experimental setup [19]. In order to reproduce the adopted data in ^{108}In, the 2^+ ground state and first excited 7^+ state of the shell model has to be interchanged. This conclusion is based on the intensity of the transition between the 3^+ state at 198 keV and the isomeric 2^+ state at 30 keV. The 3^+ state can be identified as the 262 keV state in the shell model. The shell model correctly describes the feeding of this state from above by a 4^+ state at 482 keV, corresponding to the 4^+ state at 796.4 keV in the calculation. Furthermore, both the shell model state and the experimental counterpart have a decay branch to a lower-lying second 3^+ state which then decays to the first excited isomeric 2^+ state. We stress that the coupled decay pattern of these four states is, apart from the energies of the involved states, very well reproduced in the shell model calculation. Therefore, the experimental 3^+ state at 266 keV most likely corresponds to the 501 keV state in the shell model calculation. As mentioned, the $(6, 7)^+$ at 248 keV has a 91.2% decay branch directly to the 7^+ ground state. The only similar transition in the shell model calculation is from the 5^+ state at 392 keV. Therefore the 248 keV state is here tentatively assigned as having spin and parity 5^+, see fig. 3. It should be pointed out that the 97 keV transition from the low-lying $(6, 7, 8)$ state to the 7^+ ground state was not observed since at this energy the de-excitation is dominated by internal conversion and the detection threshold of the MINIBALL Ge detectors was ~ 100 keV.

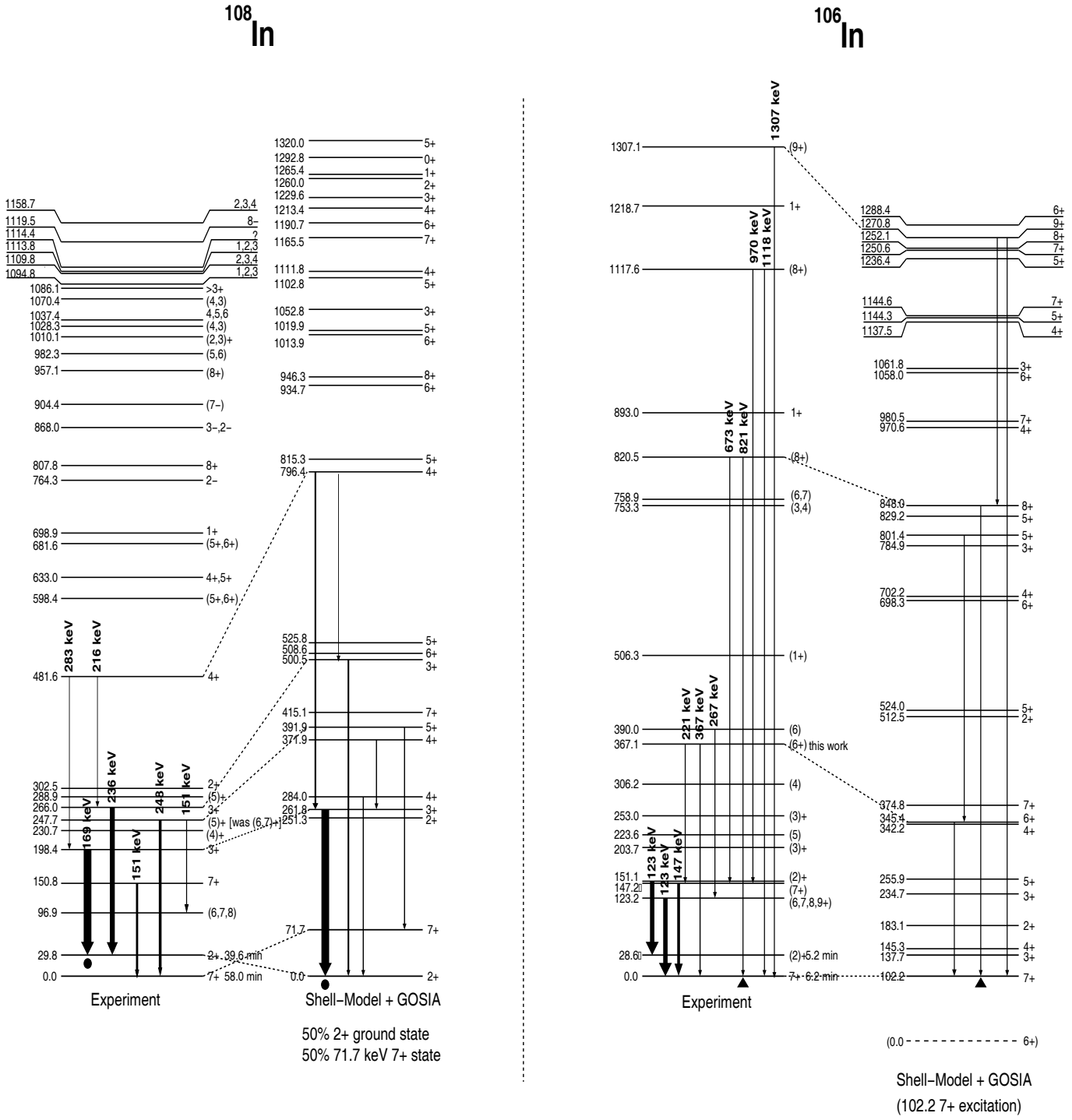

Fig. 3. Experimental and theoretical levels in ^{106,108}In. The width of the arrows reflect the observed γ-ray yields. The theoretical γ-ray de-excitation patterns were obtained from a GOSIA simulation based on the $E2$ and $M1$ transition matrix elements derived from a shell model calculation. The theoretical γ-ray yields were normalized to the experimental transition indicated with a triangle or a circle. The shell model calculation for ^{106}In predicts a 6^+ ground state and a first excited 7^+ state. In order to reproduce the experimentally observed spin sequence, the 6^+ ground state was excluded and the first excited 7^+_1 state was assigned as the ground state. The level at 367 keV in ^{106}In was observed in this work and the tentative spin assignment is indicated. Also, the experimental levels and their theoretical counterparts, where identified, are connected with a dashed line.

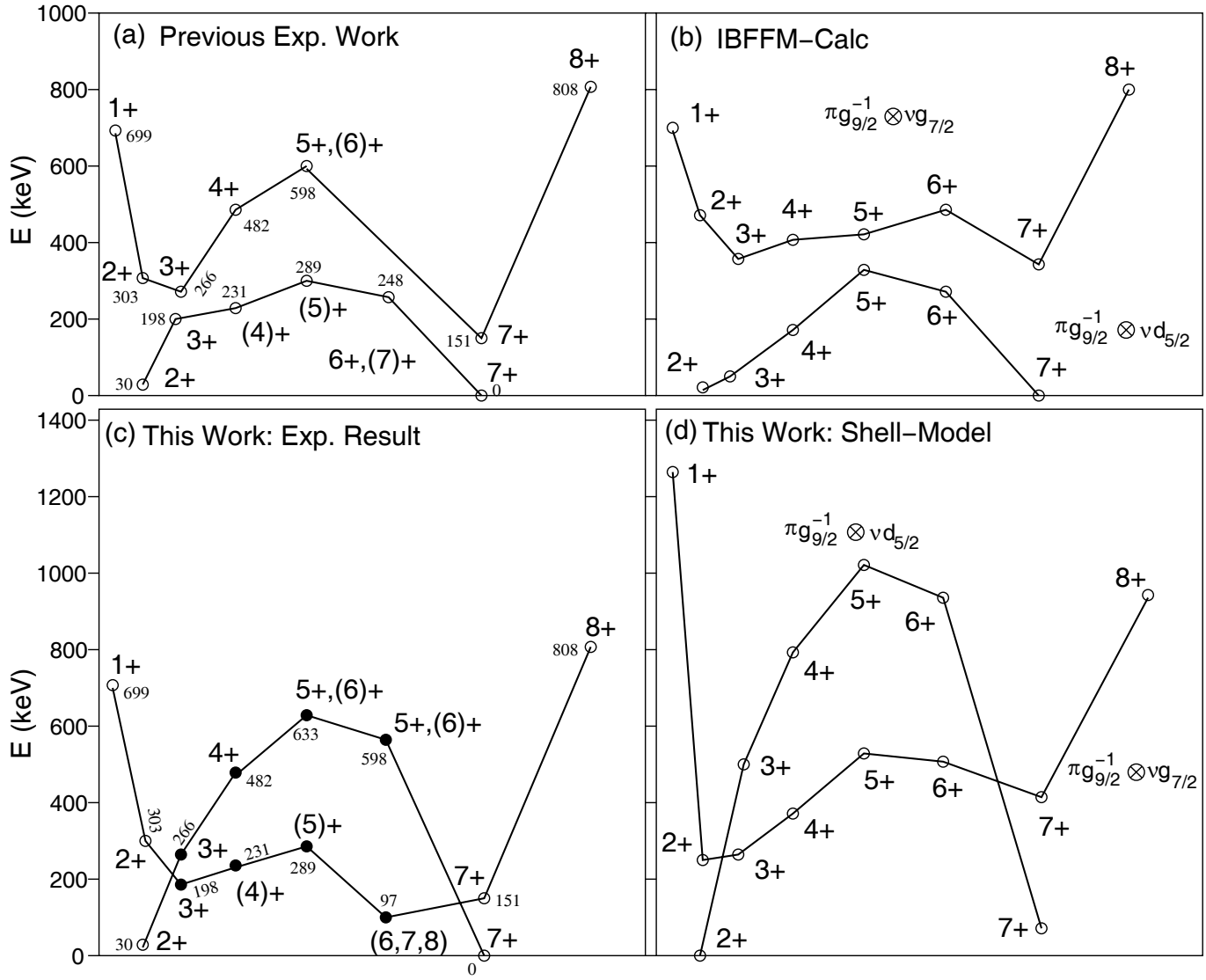

Fig. 4. The four panel show the experimental and theoretical $\pi g_{9/2}^{-1} \otimes \nu g_{7/2}$ and $\pi g_{9/2}^{-1} \otimes \nu d_{5/2}$ multiplets in ^{108}In. Empty circles (○) represent previous data or theory. Filled circles (•) represent levels re-assigned based on this work. The W-shape of the $\pi g_{9/2}^{-1} \otimes \nu g_{7/2}$ multiplet arises when the occupation probability $v_{g_{7/2}}^2 \sim 0.5$ [21]. (a) Summary of the two previous efforts [5,20] based on reaction and high-spin studies. (b) The result of the interacting-boson-fermion-fermion calculation presented in ref. [5]. (c) Multiplet interpretation of this work. (d) The multiplet structures of the shell model calculation.

3.2 Multiplet interpretation

In two previous efforts [5,20], the excited states of ^{108}In have been interpreted in terms of the $\pi g_{9/2}^{-1} \otimes \nu g_{7/2}$ and $\pi g_{9/2}^{-1} \otimes \nu d_{5/2}$ multiplets, see fig. 4(a). However, the previous measurements were not directly sensitive to the transition matrix elements but had to rely on branching and mixing ratios. These were based on decay data, angular distributions from a (p, nγ) reaction, and from a high-spin study of ^{108}In. The results were compared [5] with an interacting-boson-fermion-fermion calculation (IBFFM) [21], see fig. 4(b). The residual interaction of the corresponding Hamiltonian was fitted to reproduce the energy spectrum of ^{108}In. Here, we interpret parts of the experimental energy spectrum of ^{108}In starting from a realistic shell model interaction without phenomenological modifications, see figs. 4(c), (d). The theoretical multiplets were extracted in the following way. Between neighboring $I \rightarrow I+1$ states of the same $\pi^{-1} \otimes \nu$ multiplet one can expect a large $M1$-matrix element, which, in the following, we refer to as the $M1$-overlap. Starting with the 2^+ ground state of the shell model calculation, which has a dominating $\nu d_{5/2}$ component, a sequence of states belonging to the $\pi g_{9/2}^{-1} \otimes \nu d_{5/2}$ multiplet can be identified by following the strongest $M1$-matrix elements. Similarly, the theoretical $\pi g_{9/2}^{-1} \otimes \nu g_{7/2}$ multiplet was traced out by starting with the only 1^+ state in the shell model calculation. In detail, the 2^+ ground state of the calculation has a large $M1$-overlap with the 3^+ shell model state at 501 keV. Invoking the similarities in the simulated and observed de-

excitation patterns, it is concluded that the experimental 3^+ state at 266 keV also belongs to this multiplet, see fig. 4(c). This assumption is strengthened by this state being fed by the 4^+ state at 482 keV. This assignment differs from the one in ref. [5] and fig. 4(a). We suggest that the experimental 3^+ state at 198 keV does not belong to the $\pi g_{9/2}^{-1} \otimes \nu d_{5/2}$ multiplet. The reason is that the corresponding shell model state at 262 keV has an $M1$-overlap with respect to the 2^+ shell model ground state which is 20% smaller than the overlap with the 3^+ shell model state at 501 keV. In the previous section, the observed 4^+ state at 482 keV was identified as the calculated 4^+ state at 796 keV. The $M1$-overlap of this state with the 3^+ shell model state at 501 keV is twice that of the overlap with the 3^+ state at 262 keV. This makes a $\pi g_{9/2}^{-1} \otimes \nu d_{5/2}$ assignment of the 4^+ state at 482 keV plausible. Continuing, the 5^+ and 6^+ states of this multiplet would correspond to the shell model states at 1020 keV and 935 keV. In the shell model, these states are the fourth and the second states with these spins and parities. Therefore, assuming an equivalent sequence of the spins and parities in the experimental spectrum, the states at 633 keV and 598 keV are suggested to belong to the $\pi g_{9/2}^{-1} \otimes \nu d_{5/2}$ multiplet. In the shell model, the 6^+ state at 935 keV has the largest $M1$-overlap with the 7^+ shell model state that corresponds to the experimental ground state.

Regarding the $\pi g_{9/2}^{-1} \otimes \nu g_{7/2}$ multiplet, the only low-lying 1^+ state in the experimental spectrum is located at 699 keV. In the shell model calculation, the 1^+ state has the largest $M1$-overlap with the low-lying 2^+ state at 251 keV. The only experimental low-lying 2^+ state, apart from the isomeric state at 30 keV, is located at 303 keV. Therefore, it is reasonable to assign this state to the $\pi g_{9/2}^{-1} \otimes \nu g_{7/2}$ multiplet. From the discussion above, we assign the experimental 3^+ state at 198 keV to the $\pi g_{9/2}^{-1} \otimes \nu g_{7/2}$ multiplet. The $(4)^+$ state of this multiplet is, according to the shell model, the second state with this spin and parity. Therefore, the next non-assigned $(4)^+$ state at 231 keV is tentatively assigned to the $\pi g_{9/2}^{-1} \otimes \nu g_{7/2}$ multiplet. Similarly, the 5^+ and 6^+ states of the shell model correspond to the experimental $(5)^+$ state at 289 keV and the $(6, 7, 8)$ state at 97 keV. It is noteworthy that the 3^+-$(4)^+$-$(5)^+$ sequence of states of the $\pi g_{9/2}^{-1} \otimes \nu g_{7/2}$ multiplet were all assigned to belong to the $\pi g_{9/2}^{-1} \otimes \nu d_{5/2}$ multiplet in earlier efforts, see fig. 4(a). The lowest 7^+ and 8^+ states in the shell model calculation can be assumed to correspond to the experimental 7^+ and 8^+ states at 151 keV and 808 keV.

The $\pi^{-1} \otimes \nu$ multiplets cover the same energy range. This could be interpreted as originating in the nearly degenerate $5/2^+$ ground state and first excited $7/2^+$ state in ^{109}Sn, with an energy difference of only 13 keV [1,2]. The IBFFM calculations and the ^{108}Cd(p, nγ)^{108}In reaction data in ref. [5] predict a larger energy splitting between the $\pi g_{9/2}^{-1} \otimes \nu g_{7/2}$ and $\pi g_{9/2}^{-1} \otimes \nu d_{5/2}$ configurations than the one deduced in this work. It is worth pointing out that the parameters for the neutron-core coupling in the IBFFM calculations of ref. [5] were fitted to the energies of the experimentally determined $\pi^{-1} \otimes \nu$ multiplet.

Table 3. Observed γ-ray transitions in ^{108}In and the deduced limits on the transition probabilities where possible.

Transition	E_i (keV)	E_f (keV)	E_γ (keV)	$B(E2)$ (Wu)
$7^+ \rightarrow 7^+_{\rm gs}$	150.8	0.0	150.8	< 196
$5^+ \rightarrow 7^+_{\rm gs}$	247.7	0.0	247.7	< 222
$5^+ \rightarrow (6)$	247.7	96.9	150.8	< 93

4 Coulomb excitation analysis

For completeness we present upper limits of three $B(E2)$ values extracted from the ^{108}In data using the standard computer codes GOSIA and GOSIA2 using a ^{58}Ni target normalization. For the details regarding the normalization we refer to ref. [10]. The $E2$ and $M1$ couplings between the states shown in fig. 3 were included in the analysis as well as the small set of known branching ratios and mixing ratios from ref. [5]. For the cases where several tentative spin assignments exist, the lowest spin was chosen. However, the solution was not sensitive to any variation of tentative spin assignments for the present case. The properties of the χ^2-minimum were tested by initiating the minimization routine with a wide range of starting conditions using randomization and rescaling of the matrix elements. The statistical uncertainties of the γ-ray yields and the large number of free parameters rendered final matrix elements with large correlated uncertainties. However, the extremes of the uncertainties for three of the $E2$-matrix elements in ^{108}In were reasonable, see table 3.

5 Conclusions

In conclusion, the radioactive isotopes ^{106,108}In have been Coulomb excited from their ground states and first excited isomeric states. The multiplet structure of ^{108}In has been re-analyzed in view of the de-excitation patterns observed here. The realistic residual interaction based on the CD-Bonn potential does not predict the correct ground-state spins of ^{106,108}In but it reproduces the observed transition patterns in general. Further Coulomb excitation studies accompanied with high-statistics decay and reaction studies are needed in order to improve the precision of the transition matrix elements in ^{106,108}In. This information will provide a good benchmark for studies of the nucleon-nucleon interaction in the vicinity of ^{100}Sn, and the π-ν two-body matrix elements in particular.

This work was supported by the Swedish Research Council, the European Union through RII3-EURONS (Contract No. 506065) and the German BMBF through Grant No. 06 KY 205 I.

References

1. L. Käubler *et al.*, Z. Phys. A **351**, 123 (1995).
2. J.J. Ressler *et al.*, Phys. Rev. C **65**, 044330 (2002).
3. D. Vandeplassche *et al.*, Phys. Rev. Lett. **57**, 2641 (1986).
4. J. Eberz *et al.*, Z. Phys. A **323**, 119 (1986).
5. A. Krasznahorkay *et al.*, Nucl. Phys. A **499**, 453 (1989).
6. J. Gulyas *et al.*, Nucl. Phys. A **506**, 196 (1990).
7. B.W. Filippone *et al.*, Phys. Rev. C **29**, 2118 (1984).
8. B. Roussire *et al.*, Nucl. Phys. A **419**, 61 (1984).
9. R. Barden *et al.*, Z. Phys. A **329**, 319 (1988).
10. T. Czosnyka *et al.*, Bull. Am. Phys. Soc. **28**, 745 (1983).
11. A. Ekström *et al.*, Phys. Rev. Lett. **101**, 012502 (2008).
12. A.N. Ostrowski *et al.*, Nucl. Instrum. Methods A **480**, 448 (2002).
13. P. Reiter *et al.*, Nucl. Phys. A **701**, 209 (2002).
14. M. Hjorth-Jensen *et al.*, Phys. Rep. **261**, 125 (1995).
15. R. Machleidt *et al.*, Phys. Rev. C **53**, R1483 (1996).
16. A. Holt *et al.*, Phys. Rev. C **61**, 064318 (2000).
17. T. Kibdi *et al.*, Nucl. Instrum. Methods A **589**, 202 (2008).
18. D. Seweryniak *et al.*, Nucl. Phys. A **589**, 175 (1995).
19. A. Ekström *et al.*, Nucl. Instrum. Methods: Phys. Res. A **614**, 303 (2010).
20. C.J. Chiara *et al.*, Phys. Rev. C **64**, 054314 (2001).
21. S. Brant *et al.*, Z. Phys. A **329**, 151 (1988).